Supplementary materials for this article are available at 10.1007/s13253-010-0027-5.

Multi-Site Integrated Population Modelling

R. S. McCrea, B. J. T. Morgan, O. Gimenez, P. Besbeas, J.-D. Lebreton, and T. Bregnballe

We examine the performance of a method of integrated population modelling for the joint analysis of different types of demographic data on individuals that exist in, and move between, different sites. The value of the approach is demonstrated by a simulation study which shows substantial improvement in parameter estimation when site-specific census data are combined with demographic data. The multivariate normal approximation to a multi-state mark-recapture likelihood is evaluated, and the performance of a diagonal variance-covariance matrix for the approximation is also examined. The work is motivated by a study of great cormorants. Analysis of the cormorant data suggests that breeders survive better than non-breeders, and also that probabilities of recruitment to breeding have been declining over time for all the colonies of the study. Supplementary material, including notes on the computation of standard errors and extended simulation results, are available online.

Key Words: Great cormorant; Kalman filter; Mark-recapture data; *Phalacrocorax carbo*; Recruitment; State-space models.

1. INTRODUCTION

Mark-recapture methods are commonplace in statistical and biological research, involving probability models to estimate key demographic parameters for a variety of species. The use of mark-recapture models for survival estimation began in the 1960s, when the Cormack–Jolly–Seber model (Cormack 1964; Jolly 1965; Seber 1965) was proposed, and since then a large number of related models have been developed. One of the most prominent extensions has been the multi-site Arnason–Schwarz (AS) model (Arnason 1972;

R. S. McCrea (✉) is a Research Associate, National Centre for Statistical Ecology, School of Mathematics, Statistics and Actuarial Science, University of Kent, Canterbury, Kent CT2 7NF, England (E-mail: *r.s.mccrea@kent.ac.uk*). B. J. T. Morgan is a Professor of Applied Statistics, School of Mathematics, Statistics and Actuarial Science, University of Kent, Canterbury, Kent CT2 7NF, England. O. Gimenez is a Researcher and J.-D. Lebreton is a Research Director, Centre National de la Recherche, Centre d'Ecologie Fonctionnelle et Evolutive, UMR 5175, 1919 Route de Mende, 34293 Montpellier, France. P. Besbeas is a Research Scientist, National Centre for Statistical Ecology, University of Kent, Canterbury CT2 7NF, England and Lecturer, Athens University of Economics and Business, Athens, Greece. T. Bregnballe is a Senior Scientist, Department of Wildlife Ecology and Biodiversity, National Environmental Research Institute, Aarhus University, Kalø, 8410 Rønde, Denmark.

Journal of Agricultural, Biological, and Environmental Statistics, Volume 15, Number 4, Pages 539–561
DOI: 10.1007/s13253-010-0027-5

Arnason 1973; Schwarz, Schweigert, and Arnason 1993), which includes transition probabilities between different sites as well as survival and capture probabilities. The AS model was proposed as a unified framework for mark-recapture-recovery models by expressing the models in terms of states rather than sites (Lebreton, Almeras, and Pradel 1999), which is the framework that is used for the multi-site recapture model of this paper.

Another important development in statistical ecology is the theory of integrated modelling, which provides simultaneous analysis of related data from a variety of sources. Integrated population modelling was first proposed for the joint analysis of independent mark-recovery and census data (Besbeas et al. 2002), and allowed the coherent estimation of productivity, otherwise not estimable from either the recovery or census data alone. Since its introduction, integrated population modelling has broadened (Gauthier et al. 2007; Schaub et al. 2007; Tavecchia et al. 2009; Reynolds et al. 2009), and has been used to combine multiple data sources, including both mark-recapture and nest record data. Until now, the census data jointly modelled with demographic data have corresponded to a single site and are typically univariate. Tavecchia et al. (2009) included several census time series; however, the set of observed population counts in their application were age and sex specific, and therefore no transitions were estimated. In this paper we also analyze multivariate observations; however, the aim of the analysis differs as we estimate transition probabilities within multi-state systems.

Combining multi-state mark-recapture and census data was examined in Borysiewicz et al. (2009) for a single simulated data set. Here, we provide a general framework for multi-site integrated population modelling, we demonstrate, using both simulated and real data, the benefits of combining data in this way, and we discuss the practicality of the approach. The data which motivated the work are described in Section 2 and a resumé of multi-site mark-recapture and state-space models is given in Section 3. A simulation study exploring the potential of multi-site integrated population models is presented in Section 4, the analysis of the data set takes place in Section 5 and the paper ends with general conclusions.

2. GREAT CORMORANTS IN DENMARK

The work of this paper was motivated by data on great cormorants, *Phalacrocorax carbo*, collected by the National Environmental Research Institute in Denmark. The great cormorant is the most widely distributed of all cormorants, known to breed in North America, Europe, Asia and Australasia. The studied species belongs to the Eurasian subspecies, *P.c.sinensis*. This subspecies breeds in colonies ranging in size from a few pairs to 13,000 pairs. The subspecies usually nests in trees and shrubbery; however, on small islets, to which mammalian predators have no access, it may breed directly on the ground.

The data were collected as part of a long-term programme which took place in three colonies, Vorsø (VO), Mågeøerne (MA) and Stavns Fjord (SF). Ringing started in the main colony, VO, in 1977, and systematic searches for ringed breeders started in 1983. Ringing and searches for ringed breeders in MA and SF began in the 1980s and early 1990s, respectively. The three colonies were founded in 1944, 1985 and 1989, respectively and are

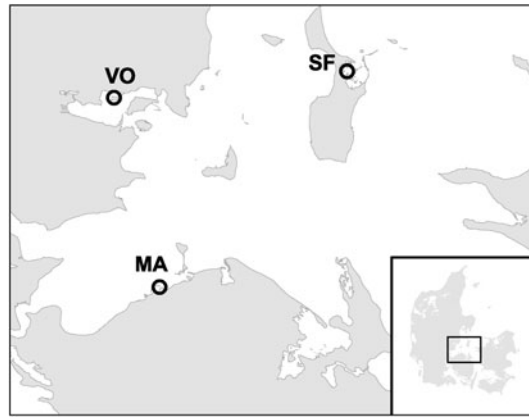

Figure 1. Map of the three Danish cormorant colonies: Vorsø (VO), Mågeøerne (MA) and Stavns Fjord (SF).

located in an extensive shallow area of southwestern Kattegat (Figure 1). We analyze the data collected on individuals between 1991 and 2004.

Chicks, mostly aged between 25 and 38 days, were ringed using a standard metal ring on one leg, and a colored plastic ring with a unique combination of three alphanumeric characters on the other. Resightings of colour-ringed individuals, during breeding attempts, were conducted from towers, hides and directly from the ground at a distance using a telescope. The birds do not start breeding before they are 2 years or older (Frederiksen, Lebreton, and Bregnballe 2001), and for the present analyses only resightings of individuals recorded as breeders or presumed breeders are available.

Colony size was estimated during each year of the study by counting the number of nests in early May, which is the time of year when nest numbers peak. We use the figures from 1991–2004, which are plotted in Figure 5. The marked individuals at each colony make up a small proportion of the censused population; thus, the risk of biasing the parameter estimates (Besbeas, Borysiewicz, and Morgan 2009) or experiencing overly optimistic levels of precision due to dependencies between data sets is low.

Hénaux, Bregnballe, and Lebreton (2007) analyzed a six-colony cormorant data set and estimated the transitions of interest by using a multi-state mark-recapture model alone, and their results will be discussed in Section 5. The work of this paper is the first time that the cormorant census data have been modelled in conjunction with the recapture data, providing a coherent model for the entire studied population.

3. INTEGRATED MODELS FOR INDEPENDENT MULTI-SITE MARK-RECAPTURE AND CENSUS DATA

3.1. THE ARNASON–SCHWARZ MODEL

The AS model can be applied to multi-site mark-recapture data in order to estimate three important sets of biological parameters: survival probabilities, transition probabilities and capture probabilities. The general parameter notation of the AS model is:

$\phi_t(r)$: The probability that an individual alive in state r at time t survives until time $t+1$.

$\psi_t(r,s)$: The probability that an individual in state r at time t moves to state s by time $t+1$, given that the individual survives the time period t to $t+1$.

$p_{t+1}(s)$: The probability that an individual in state s at time $t+1$ is recaptured at this time.

Multi-site mark-recapture data can be summarized in an array form, where $m_{ij}(r,s)$ denotes the number of individuals released at time i in state r and next recaptured at time j in state s. For given i and r, the vector of observations $m_{i\cdot}(r,\cdot)$ can be modelled by a multinomial distribution, constructed in terms of the three parameter types defined above. The overall likelihood is product-multinomial in form, as a result of multiplication of the multinomial components over all possible values of i and r (Williams, Nichols, and Conroy 2001, p. 456).

The transitions defined here are first-order Markov movements so that individuals' movements depend only on current location and no memory is modelled. These assumptions have been relaxed (Brownie et al. 1993); however, for the integrated population modelling presented within this paper, the first-order Markov transitions are sufficient for both the AS and state-space model components.

3.2. THE STATE-SPACE MODEL

State-space models are a specific case of a wider class of models known as hidden-process models (Newman et al. 2006). The state-space form applies to a multivariate time series where $\mathbf{y}_1, \mathbf{y}_2, \ldots, \mathbf{y}_N$ are $m \times 1$ vectors. These observable variables are related to a $u \times 1$ vector $\boldsymbol{\alpha}_t$ known as the state vector via an *observation equation* given by Equation (3.1),

$$\mathbf{y}_t = \mathbf{Z}_t \boldsymbol{\alpha}_t + \boldsymbol{\epsilon}_t \quad \text{for } t = 1, \ldots, N, \tag{3.1}$$

where $\mathbf{Z}_t$ is an $m \times u$ matrix and $\boldsymbol{\epsilon}_t$ is an $m \times 1$ vector of serially uncorrelated random variables with mean zero, $\mathrm{E}(\boldsymbol{\epsilon}_t) = 0$ and covariance matrix, $\mathrm{var}(\boldsymbol{\epsilon}_t) = \mathbf{H}_t$.

In general, the elements of $\boldsymbol{\alpha}_t$ are not observable; however, they are assumed to be generated by a first-order Markov process defined by Equation (3.2) and referred to as the *state equation*,

$$\boldsymbol{\alpha}_{t+1} = \mathbf{T}_t \boldsymbol{\alpha}_t + \boldsymbol{\eta}_t. \tag{3.2}$$

Here $\mathbf{T}_t$ is a $u \times u$ population projection matrix and $\boldsymbol{\eta}_t$ is a $u \times 1$ vector of serially uncorrelated random variables over time with mean zero, $\mathrm{E}(\boldsymbol{\eta}_t) = 0$, and covariance matrix, $\mathrm{var}(\boldsymbol{\eta}_t) = \mathbf{Q}_t$.

The specification of a Gaussian state-space system is obtained by two further assumptions:

(i) The initial state vector $\boldsymbol{\alpha}_1$ has mean $\mathbf{a}_1$ and covariance matrix $\mathbf{P}_1$, such that $\boldsymbol{\alpha}_1 \sim N(\mathbf{a}_1, \mathbf{P}_1)$.

(ii) The random variables $\boldsymbol{\epsilon}_t$ and $\boldsymbol{\eta}_t$ are uncorrelated with each other in all time periods, and uncorrelated with the initial state, that is $\mathrm{E}(\boldsymbol{\epsilon}_t \boldsymbol{\eta}_s') = 0$, $\forall s, t = 1, \ldots, N$ and $\mathrm{E}(\boldsymbol{\epsilon}_t \boldsymbol{\alpha}_1') = 0$, $\mathrm{E}(\boldsymbol{\eta}_t \boldsymbol{\alpha}_1') = 0$, for $t = 2, \ldots, N$, where $\boldsymbol{\epsilon}_t \sim N(0, \mathbf{H}_t)$ and $\boldsymbol{\eta}_t \sim N(0, \mathbf{Q}_t)$.

It is the Gaussian assumptions defining the system which allow the implementation of a recursive estimation procedure known as the Kalman filter (Harvey 1989; Durbin and Koopman 2001) for model fitting by maximum likelihood. From the Kalman filter, the conditional distribution of $\boldsymbol{\alpha}_{t+1}$ given $\{\mathbf{y}_1, \ldots, \mathbf{y}_t\}$ can be constructed and a likelihood function for the unknown parameters within the model can be formed. After filtering, it is then possible to 'smooth' the estimates, which involves computing the estimates $\boldsymbol{\alpha}_{t+1}$ conditional on all of the available data, $\{\mathbf{y}_1, \ldots, \mathbf{y}_N\}$. In the general state-space modelling literature, the state vector is defined to be the smallest subset of system variables that can represent the entire state of the system at any time. For ecological applications, the state vector $\boldsymbol{\alpha}_t$ is generally structured in terms of age-classes of individuals (Buckland et al. 2004), which can also be location-specific.

In order to initiate the Kalman filter, it is necessary to provide a starting value for the initial state vector $\boldsymbol{\alpha}_1$. One proposal for integrated population models is to take the mean vector $\mathbf{a}_1$ to be proportional to the stable-age distribution of an appropriate population projection matrix $\mathbf{T}$, with the proportions scaled by the total size of the first observation. The maximum-likelihood estimates (MLEs) for the stable-age calculation with respect to the population projection matrix can be obtained from the analysis of the mark-recapture data alone. Parameters not estimated from the mark-recapture data can be estimated iteratively; see Besbeas and Morgan (2010) and Besbeas, Borysiewicz, and Morgan (2009).

For ecological applications the covariance matrix is $\mathbf{Q}_t$ with binomial and Poisson entries as appropriate in terms of the expected values of the unknown states, as suggested for single-site applications in Besbeas et al. (2002). Also, we suppose that $\mathbf{H}_t$ is a diagonal matrix with entries σ. It is possible that σ, termed the observation error, may depend on state and/or time.

Deterministic matrix models such as those presented in Caswell (2000) develop from specific starting values for all states within the state vector. In contrast, state-space modelling is not only stochastic, but there are also mechanisms to perform the iterative model-fitting procedure even under diffuse initial state vectors. Further, it is possible to obtain smoothed estimates of the entries in the unknown state vector, compared to deterministic approaches which would only mimic the observed counts.

3.3. INTEGRATING THE MODELS

The key concept behind integrated population modelling is that the available sources of data contain information on common parameters. In the context of the cormorant application, the recapture data contain information on survival, ϕ, transition, ψ, and capture, p, parameters, while the census data contain information on survival, ϕ, and transition, ψ, parameters as well as on the additional parameters fecundity, f, and observation error, σ. Suppose the likelihood function from the recapture data alone is denoted by $\mathbf{L}_R(\phi, \psi, p)$

and the likelihood function arising from the census data is denoted by $\mathbf{L}_C(\phi, \psi, f, \sigma)$. Then, rather than maximizing each likelihood separately, assuming independence a global likelihood, denoted by $\mathbf{L}_G(\phi, \psi, p, f, \sigma)$, containing the information from both data sets, can be optimized to provide global MLEs,

$$\mathbf{L}_G(\phi, \psi, p, f, \sigma) = \mathbf{L}_R(\phi, \psi, p) \times \mathbf{L}_C(\phi, \psi, f, \sigma). \tag{3.3}$$

The potential for improved estimates from the global likelihood derives from the potentially greater effective sample size of the aggregate data. A practical difficulty of this approach is that there is a lack of flexible software for fitting both components of the likelihood simultaneously. Further, many researchers may only be able to obtain multi-state capture-recapture parameter estimates through the use of specialized software such as Program MARK (White and Burnham 1999) or M-Surge (Choquet et al. 2004) or even through literature searches.

As a consequence, it may be difficult to form the global likelihood. Besbeas, Lebreton, and Morgan (2003) showed that a multivariate normal approximation to a mark-recovery likelihood function may be used in place of the explicit mark-recovery likelihood function. This approach is motivated by the asymptotic distribution of the MLE and has been found to work well for single-site mark-recovery data. Denoting the parameters in the mark-recapture model by $\boldsymbol{\theta}$, this approximation is based on the MLE from the mark-recapture analysis, $\hat{\boldsymbol{\theta}}$, and the corresponding estimated variance-covariance matrix, $\hat{\boldsymbol{\Sigma}}$, and is given by

$$\log \mathbf{L}_{\mathbf{R}}(\boldsymbol{\theta}) \approx \text{constant} - \frac{1}{2}\big(\hat{\boldsymbol{\theta}} - \boldsymbol{\theta}\big)' \hat{\boldsymbol{\Sigma}} \big(\hat{\boldsymbol{\theta}} - \boldsymbol{\theta}\big). \tag{3.4}$$

The performance of this approximation for multi-site mark-recapture modelling is examined using simulation in Section 4.2.

4. SIMULATION STUDY

A simulation study based on the cormorant data set was carried out to illustrate the potential of multi-site integrated population modelling and investigate its performance with respect to using both multivariate census observations and the multivariate normal approximation. This study extends the work in Borysiewicz et al. (2009), enabling more general conclusions and observations to be made, and we shall mention their findings later.

Data were simulated from a population with three sites, which we label A, B and C. Mark-recapture data were simulated for a period of 5 release years and 5 recapture years, and census data spanned 25 years. The 5 release years and subsequent recapture years coincided with the first 5 years of the census data. Recapture data represent adult individuals only; however, for the census simulation a two-age class structure consisting of individuals in their first year of life and adults is assumed. These values were chosen to assess the information contained in a relatively short (and generally expensive to coordinate) mark-recapture experiment, and a more lengthy census experiment. The data were simulated assuming a constant fecundity, and a recapture probability depending linearly on time on

the logistic scale. The survival probabilities were assumed to vary with a simulated time-dependent covariate (obtained from a MATLAB random number generator prior to the full simulation run) but were constant over site; the transition parameters were constant over time but were dependent on both departure and arrival sites. The observation error was set to be constant over site and time. The parameter values used for this simulation are given within the Web Appendix. The population projection matrix governing the underlying state process is given by:

$$\mathbf{T}_t = \begin{pmatrix} 0 & 0 & 0 & \phi_t f & 0 & 0 \\ 0 & 0 & 0 & 0 & \phi_t f & 0 \\ 0 & 0 & 0 & 0 & 0 & \phi_t f \\ \phi_t & 0 & 0 & \phi_t \psi(A,A) & \phi_t \psi(B,A) & \phi_t \psi(C,A) \\ 0 & \phi_t & 0 & \phi_t \psi(A,B) & \phi_t \psi(B,B) & \phi_t \psi(C,B) \\ 0 & 0 & \phi_t & \phi_t \psi(A,C) & \phi_t \psi(B,C) & \phi_t \psi(C,C) \end{pmatrix}$$

where the parameters follow the notation of Section 3. The corresponding state vector $\boldsymbol{\alpha}_t$ is given by

$$\left(N^1(A) \quad N^1(B) \quad N^1(C) \quad N^{2+}(A) \quad N^{2+}(B) \quad N^{2+}(C)\right)'_t$$

where $N_t^a(r)$ denotes the number of age a animals in state r at time t. Thus from this structure, the mark-recapture model contained 10 parameters, whilst the integrated mark-recapture and census model contained 12 parameters. The summary results presented below are a small selection from a larger set of simulation runs (see the Web Appendix for further details).

4.1. EXPLORING THE POTENTIAL OF MULTIVARIATE CENSUS DATA

The primary motivation for performing single-site integrated population modelling has been the estimation of parameters not estimable from either data set alone along with a measure of standard error (SE). This is because, in the case of single-site census data, models are often parameter redundant, and in these circumstances it would not be possible to estimate fecundity from the census data alone. We note here that the identifiability of parameters within a state-space model will depend on the structure of the parameters within the population projection matrix. The model we have simulated above assumes that survival is time dependent but not age dependent, and as a result none of the parameters is confounded with one another. Interestingly, in the case of multi-site census data it is sometimes possible to estimate parameters which would not be identifiable if only univariate census data were available. However associated SEs are likely to be very large from census data alone. The simulation study was carried out to investigate this and to estimate both bias and SEs. In addition, in order to gauge the difference between multivariate and univariate census information, we consider site-specific census data as well as census data pooled over the three sites. To model these two scenarios we consider two alternative observation equations:

$$y_t = (0 \quad 0 \quad 0 \quad 1 \quad 1 \quad 1)\boldsymbol{\alpha}_t + \epsilon_t \tag{4.1}$$

Table 1. Bias and SE estimates from 100 simulations comparing recapture data alone, census data alone, joint recapture and site-specific census data and joint recapture and pooled census data.

	Recapture alone		Census alone[a]		Recapture and census		Recapture and pooled census	
Parameter	Bias	SE	Bias	SE	Bias	SE	Bias	SE
ϕ_{int}	0.024	0.197	−0.005	0.191	0.004	0.064	0.003	0.063
ϕ_{slope}	−0.030	0.348	0.026	0.128	0.004	0.079	0.004	0.078
$\psi(A, B)$	0.012	0.216	1.131	2.465	0.012	0.196	0.012	0.216
$\psi(A, C)$	0.002	0.175	0.088	2.298	−0.006	0.151	0.002	0.175
$\psi(B, A)$	−0.016	0.230	−0.548	2.745	0.012	0.197	−0.016	0.229
$\psi(B, C)$	0.000	0.190	−1.896	2.492	0.002	0.157	0.000	0.190
$\psi(C, A)$	−0.040	0.190	−0.291	2.303	−0.010	0.163	−0.040	0.190
$\psi(C, B)$	−0.024	0.179	−0.964	3.180	−0.004	0.154	−0.024	0.179
p_{int}	0.003	0.099			0.002	0.097	0.004	0.098
p_{slope}	−0.021	0.221			−0.010	0.192	−0.008	0.192
f			−0.010	0.310	−0.010	0.082	−0.007	0.082
σ			−0.134	0.184	−0.038	0.165		

[a]Note that averages are only across the 31 census-only simulations which contained no boundary estimates; see text for further details.

and

$$\mathbf{y}_t = \begin{pmatrix} 0 & 0 & 0 & 1 & 0 & 0 \\ 0 & 0 & 0 & 0 & 1 & 0 \\ 0 & 0 & 0 & 0 & 0 & 1 \end{pmatrix} \boldsymbol{\alpha}_t + \boldsymbol{\epsilon}_t. \tag{4.2}$$

Thus observation equation (4.1) has pooled site-specific census data and will result in a univariate time series, whilst observation equation (4.2) models the site-specific information. Through these models we are able to assess the benefits of incorporating a multivariate time series of population observations.

Figure 2 shows boxplots of the MLEs, and Table 1 gives the values of average bias and SEs (resulting from inverting a numerical approximation to the Hessian matrix at the MLE) of the parameter estimates over 100 simulations from analyzing the:

(1) Recapture data alone

(2) Census data alone

(3) Recapture and site-specific census data

(4) Recapture and pooled census data.

We can see that the estimates from census data alone have large SEs and large bias. This is because typically the census likelihood is relatively flat and it can be a difficult surface to optimize. Of the 100 simulations run, 69 contained boundary estimates and hence it was not possible in these cases to provide estimates of SE. These 69 simulation runs were excluded from the census data alone values in Table 1. From the census data alone, however, we are still able to estimate fecundity and observation error. The parameter structure of the state-space model used here is therefore not parameter redundant, unlike the single-site state space model considered in Besbeas et al. (2002); we see this from the entries of $\mathbf{T}_t$.

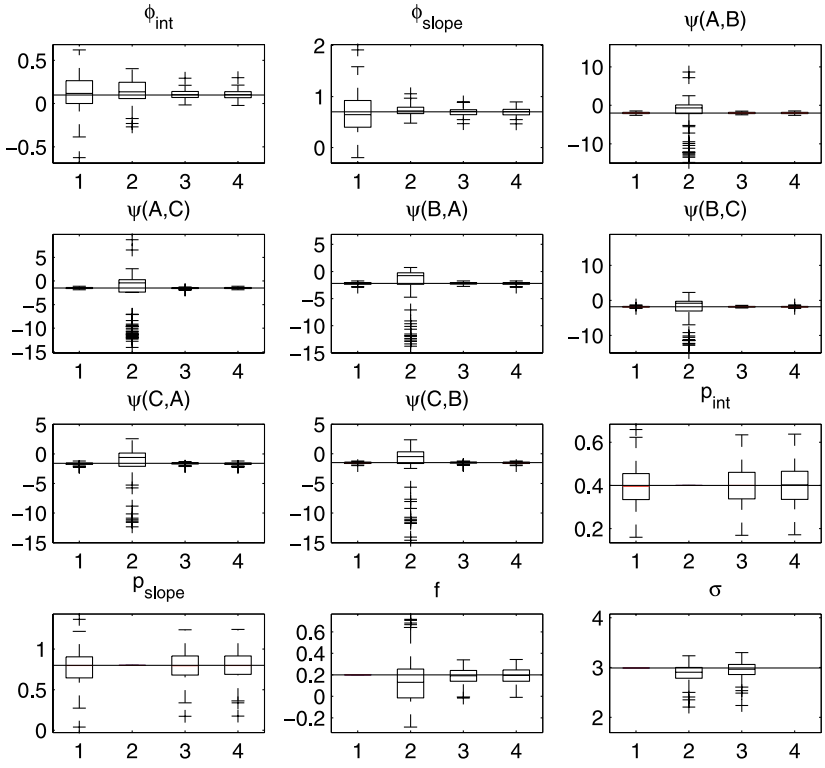

Figure 2. Boxplots of the maximum likelihood estimates from the four modelling approaches. 1: Recapture data alone; 2: census data alone; 3: recapture and site-specific census data; 4: recapture and pooled census data. The true value of the parameter is presented on each figure.

Except for the survival parameters, the 5 years of recapture data provide better estimates compared to the 25 years of census data alone. When census data are integrated with the recapture data, estimation performance improves appreciably compared to the separate analyses. A particularly strong improvement is observed in the survival parameters. However, the transition probabilities also demonstrate a decrease in SE. This is noteworthy because transition probabilities are typically difficult to estimate precisely. The precision of fecundity is also strongly improved when the recapture data are included in the analysis even though recapture data contain no information on this parameter. This is most likely due to the improved estimation of the parameters correlated with fecundity.

When we compare the two integrated analyses, we observe that pooling the census data results in less improvement in the estimation of the transition parameters compared to not pooling. However, the estimation of survival, capture and fecundity seems largely unaffected. The multi-site information has therefore improved the estimation of the site-specific parameters.

Table 2. Bias and SE estimates from 100 simulations comparing exact recapture and census model, the approximate recapture and census model and the diagonal approximate recapture and census model.

	Bias			SE		
	Exact	Approximation	Diagonal approximation	Exact	Approximation	Diagonal approximation
ϕ_{int}	0.005	0.002	0.010	0.063	0.064	0.138
ϕ_{slope}	0.002	−0.000	0.001	0.078	0.078	0.106
$\psi(A, B)$	0.017	0.020	0.021	0.196	0.197	0.194
$\psi(A, C)$	−0.006	−0.003	−0.004	0.151	0.151	0.148
$\psi(B, A)$	0.016	0.019	0.019	0.196	0.199	0.196
$\psi(B, C)$	0.006	0.009	0.007	0.157	0.157	0.154
$\psi(C, A)$	−0.009	−0.005	−0.006	0.162	0.164	0.160
$\psi(C, B)$	−0.005	−0.001	−0.004	0.154	0.155	0.151
p_{int}	0.004	0.008	0.005	0.097	0.097	0.099
p_{slope}	−0.009	−0.005	−0.024	0.192	0.192	0.221
f	−0.009	−0.004	−0.013	0.082	0.082	0.222
σ	−0.036	−0.036	−0.037	0.165	0.165	0.166

4.2. EVALUATION OF THE MULTIVARIATE NORMAL APPROXIMATION TO MULTI-SITE LIKELIHOODS

Besbeas, Lebreton, and Morgan (2003) found that a multivariate normal approximation to their mark-recovery component likelihood could be used successfully in their examples. The performance of the approximation was not assessed using simulation, however. In this section we extend the approximation to multi-site mark-recapture likelihoods and evaluate its performance using simulation. We also consider the effects of using a diagonal variance-covariance matrix within the multivariate normal approximation. This is important in practice since typically what are reported by authors are only MLEs and SEs from their analysis, and if diagonal variance-covariance matrices are seen to perform adequately, then many data sets from existing publications may be combined for integrated modelling.

Table 2 shows the average bias and SE of the estimates from:

(1) Exact recapture and multivariate census model

(2) Full approximate recapture and multivariate census model

(3) Diagonal approximate recapture and multivariate census model.

The full approximate recapture likelihood performs well for all parameters in terms of bias and SE. We observe that for the transition and recapture parameters the three models provide similar precision values. However, the diagonal approximate recapture likelihood performs less well for the survival parameters. Recall that the survival parameters are coefficients of a logistic regression of a time-dependent covariate. The recapture data alone provide only 5 years of data, and it is unsurprising that these parameters are estimated poorly when all correlations with other parameters have been ignored. Similarly, the fecundity estimate from this model has increased bias and more conservative SEs due to the lack of correlation structure.

Figure 3 shows profile mark-recapture log-likelihood plots for the intercept parameter ϕ_{int} and $\psi(A, C)$ parameter from a typical replication; the profiles are taken with respect

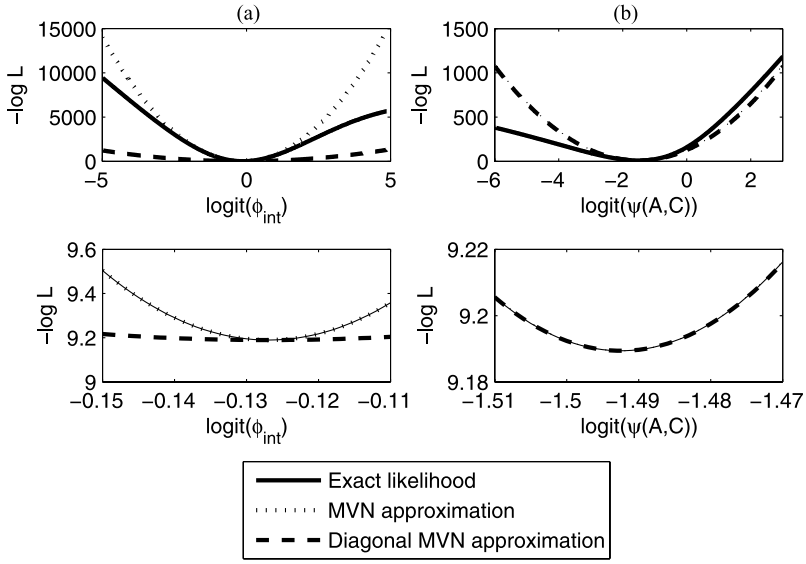

Figure 3. Profile log-likelihood plots with respect to (a) logit(ϕ_{int}) and (b) logit($\psi(A, C)$) of the exact mark-recapture likelihood, the multivariate normal approximation (MVN) to the mark-recapture likelihood and the MVN constructed using the diagonal variance-covariance matrix.

to the remaining parameters in the model. Although both approximations look reasonable near the minimum, for the ϕ_{int} parameter, the diagonal approximation quickly diverges as the parameter moves away from the MLE, and the plots look different overall. So although at first assessment we might conclude that the diagonal multivariate normal approximation will not function well in an integrated framework, it is the behavior around the minimum that will affect its performance.

The multivariate normal approximation is based on an asymptotic relationship, and therefore is always going to be better when more data are available. The plots presented in this section have been from simulations with relatively small numbers of marked individuals (1,500 in this instance), recaptured for a short time period. The mark-recapture data contain very little information on ϕ_{int} due to the short time period for which the data are available. Therefore, the diagonal multivariate normal approximation does not have a very close fit to the exact likelihood for this parameter. However, since the transitions are constant over time, both approximations perform well for the $\psi(A, C)$ parameter.

When the recapture likelihoods are combined with the census likelihood, the integrated MLE is likely to be close for both approximations. However, when estimating SEs or confidence intervals, there are likely to be some differences between the two approximations for the ϕ_{int} parameter due to the different behavior around the MLE. This is evident from the entries in Table 2.

5. GREAT CORMORANT DATA ANALYSIS

5.1. MODEL STRUCTURE

From the nature of the data described in Section 2, it is clear for this application that the transition structure of the required model is complex. As well as geographical movements, transitions representing movement between the biological states of non-breeder and breeder are of interest. We define nine states:

Newly marked non-breeders, $\{x_1\colon\ vo_1, ma_1, sf_1\}$

Established non-breeders, $\{x\colon\ vo, ma, sf\}$

Breeders, $\{X\colon\ VO, MA, SF\}$.

We define the following transitions of interest:

Breeding dispersal, (transition from X to X)

Recruitment, (transition from x to X)

Natal dispersal, (transition from x_1 to x)

Non-maturation, (transition from x to x).

Cormorants are marked as juvenile non-breeders and not recaptured until they have become breeding individuals; thus the established non-breeder state, x, is unobservable. Because of this, it is necessary to impose a number of constraints in order to make the natal dispersal and recruitment transitions identifiable. The assumptions made are:

- Newly marked cormorants remain non-breeders for at least two years after marking.
- Natal dispersal occurs only during the first year after marking of an individual. Once that year has passed, the individual remains in that site until it has recruited to a breeding state, and as such recruitment does not occur between sites.
- Once individuals have entered a breeding state, they remain in the breeding state until death.
- It is assumed that no emigration occurs out of the studied colonies.

For clarity, the state and site transitions are presented in Figure 4. Within this analysis it is assumed that the population is closed to emigration. If emigration were to occur, the estimates of survival within this analysis would represent apparent survival, as opposed to true survival. Previous analyses of related colonies of cormorants found that the emigration of individuals to areas outside of the studied colonies was very low (Borysiewicz 2008; McCrea, Morgan, and Bregnballe 2009). A key problem of emigration estimation within integrated population modelling is the identifiability of parameters. Had recovery data been available for this data set, it would have been possible to estimate emigration rates as proposed in Hénaux, Bregnballe, and Lebreton (2007); however, not all parameters were identifiable for integrated population models including emigration when recovery data were not available (further details are given in Borysiewicz 2008).

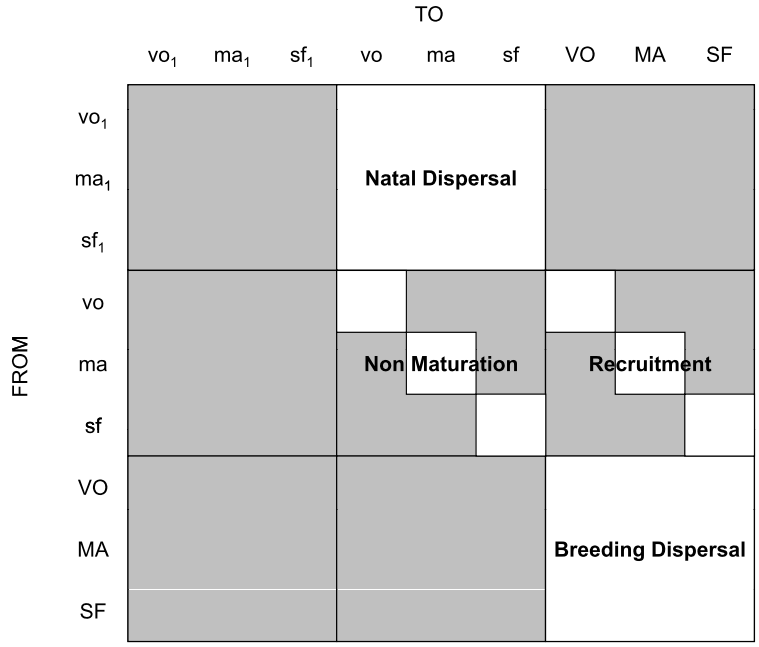

Figure 4. Diagram of transitions between newly marked non-breeding states (vo_1, ma_1,sf_1), established non-breeding states (vo, ma, sf) and breeding states (VO, MA, SF). Transitions shaded in grey are constrained to zero. It is assumed that the population is closed, and all rows of transitions must sum to 1, thus the non-maturation probabilities are constrained to be the complement of the recruitment probabilities.

Define $N_{z,t}$ to be the number of non-breeding cormorants in site z at time t, whilst $B_{z,t}$ denotes the number of breeding cormorants in site z. Then the unobserved state vector can be defined to be

$$\boldsymbol{\alpha}_t = (N_{VO} \quad N_{MA} \quad N_{SF} \quad B_{VO} \quad B_{MA} \quad B_{SF})_t.$$

Following the notation of Equation (3.1), since only breeders are observed,

$$\mathbf{Z}_t = \begin{pmatrix} 0 & 0 & 0 & 1 & 0 & 0 \\ 0 & 0 & 0 & 0 & 1 & 0 \\ 0 & 0 & 0 & 0 & 0 & 1 \end{pmatrix}, \qquad \forall t.$$

We can write the observation variance matrix, H_t, as a diagonal matrix with entries denoted by $\sigma_{z,t}$.

5.2. MODEL SELECTION

Preliminary model selection was conducted for the mark-recapture component data set alone to provide an informed starting point for the integrated model selection. Mark-recapture models were fitted using software M-Surge. Multi-site goodness-of-fit tests were conducted in U-Care (Choquet et al. 2003) and the estimated over-dispersion coefficient was $\hat{c} = 2.24$, indicating moderate over-dispersion of the data compared to the fitted model.

As a result, the AIC was corrected for lack of fit (QAIC) when used for model selection (Burnham and Anderson 2002).

A step-wise model selection procedure was implemented using QAIC as the discriminatory measure. An alternative would have been the use of a score test procedure (McCrea and Morgan 2010); however, at present this is not possible within software M-Surge.

The mark-recapture model identified by the model selection procedure involved 45 parameters with demographic parameters structured as follows:

- Site- and state-dependent survival probabilities, denoted by $\phi(from * state)$
- Constant breeding dispersal, denoted by $B(\cdot)$
- Arrival site-dependent natal dispersal, denoted by $N(to)$
- Time- and site-dependent capture probabilities, denoted by $p(to * time)$
- Time-trend recruitment probabilities, denoted by $R(T)$.

The structure of the mark-recapture component data set became the basis for the construction of the population projection matrix of the state-space model for the census data. The state-space model also contained additional parameters, denoting fecundity and observation error, f and σ, respectively.

The model selection strategy for the integrated model could not be based on QAIC since it is not possible to estimate the over-dispersion of the joint model. Therefore, the 45 parameter model was used as a starting point for model selection for the joint analysis; however, the measure used to assess the suitability of the joint models was the AIC. Model selection of the integrated recapture and census model was then conducted on a specified model set which consisted of additional time, site and state dependencies within appropriate parameters, as well as testing models with parameter dependencies removed. A selection of the integrated population models fitted is presented in Table 3 ranked in increasing value of AIC.

When fitting state-space models one must be aware of the risk of fitting overparameterized models to the data. Such overfitted models result in estimated observation errors of zero, and can cause incorrect decisions to be made within model-selection procedures (Besbeas and Morgan 2009). For this reason models with estimated observation errors of zero are excluded from Table 3.

The model with the smallest AIC was found to be $\phi(from * state + time)$, $B(from * to)$, $N(to)$, $R(from + T)$, $f(site)$, $\sigma(\cdot)$; however, when performing a likelihood-ratio test, the additional site dependence within the breeding dispersal parameter was found to be non-significant ($p = 0.07$). Therefore, we select $\phi(from * state + time)$, $B(from)$, $N(to)$, $R(from + T)$, $f(site)$, $\sigma(\cdot)$ as an appropriate model for discussion.

5.3. Results

Figure 5 shows observed breeding bird census counts and the smoothed fitted curve resulting from the chosen integrated population model. The figure also displays estimates of the non-breeding counts at each of the sites ($\hat{N}_{z,t}$, $z = 1, 2, 3$), obtained from the smoothing process.

Table 3. Integrated population models ranked by AIC(−1900). Here ϕ denotes survival, R denotes recruitment, B denotes breeding dispersal, N denotes natal dispersal, f denotes the fecundity parameter and σ denotes the observation error. n denotes the number of parameters. The parameter dependencies are denoted by: *from*: departure-site, *to*: arrival-site, *time*: time, T: regression over linear time-trend, *site*: current site, *state*: non-breeder/breeder state. $*$ denotes an interaction whilst $+$ denotes an additive effect.

Model	n	AIC	ΔAIC
$\phi(from * state + time)$, $B(from * to)$, $N(to)$, $R(from + T)$, $f(site)$, $\sigma(\cdot)$	70	13.2	0.0
$\phi(from * state + time)$, $B(from)$, $N(to)$, $R(from + T)$, $f(site)$, $\sigma(\cdot)$	67	14.4	1.2
$\phi(from * state + time)$, $B(to)$, $N(to)$, $R(from + T)$, $f(site)$, $\sigma(\cdot)$	67	16.4	3.2
$\phi(from * state + time)$, $B(from)$, $N(from * to)$, $R(from + T)$, $f(site)$, $\sigma(\cdot)$	70	16.9	3.8
$\phi(from * state + time)$, $B(\cdot)$, $N(to)$, $R(from + T)$, $f(site)$, $\sigma(\cdot)$	65	19.0	5.8
$\phi(from * state + time)$, $B(\cdot)$, $N(from * to)$, $R(from + T)$, $f(site)$, $\sigma(\cdot)$	68	21.5	8.4
$\phi(from * state + time)$, $B(\cdot)$, $N(to)$, $R(from + T)$, $f(\cdot)$, $\sigma(\cdot)$	63	27.7	14.5
$\phi(from * state + time)$, $B(\cdot)$, $N(from * to)$, $R(from + T)$, $f(\cdot)$, $\sigma(\cdot)$	66	29.8	16.6
$\phi(from * state + time)$, $B(\cdot)$, $N(to)$, $R(T)$, $f(\cdot)$, $\sigma(\cdot)$	61	51.8	38.6
$\phi(from * state)$, $B(\cdot)$, $N(to)$, $R(from + T)$, $f(\cdot)$, $\sigma(\cdot)$	49	54.7	41.6
$\phi(from * state)$, $B(\cdot)$, $N(from * to)$, $R(T)$, $f(\cdot)$, $\sigma(\cdot)$	50	70.0	56.8
$\phi(from * state)$, $B(\cdot)$, $N(to)$, $R(T)$, $f(site)$, $\sigma(\cdot)$	49	79.4	66.2
$\phi(from * state)$, $B(from)$, $N(to)$, $R(T)$, $f(\cdot)$, $\sigma(\cdot)$	49	80.9	67.8
$\phi(from * state)$, $B(to)$, $N(to)$, $R(T)$, $f(\cdot)$, $\sigma(\cdot)$	49	81.5	68.3
$\phi(from * state)$, $B(\cdot)$, $N(to)$, $R(T)$, $f(\cdot)$, $\sigma(\cdot)$	47	82.4	69.3
$\phi(from * state)$, $B(\cdot)$, $N(to)$, $R(T)$, $f(\cdot)$, $\sigma(site)$	49	82.5	69.3
$\phi(from * state)$, $B(\cdot)$, $N(to + time)$, $R(T)$, $f(\cdot)$, $\sigma(\cdot)$	61	84.0	70.8
$\phi(from * state)$, $B(time)$, $N(to)$, $R(T)$, $f(\cdot)$, $\sigma(\cdot)$	61	85.5	72.4

The MLEs (on the logistic/log scale) and corresponding SEs from the mark-recapture data alone and the combined mark-recapture and census data are presented in Table 4. The parameter estimates are similar, indicating the compatibility of the two data sets and there is appreciable improvement in the precision of most parameters, as was expected from the earlier simulation results. The fecundity parameter MLEs ($f(VO) = 1.60$ (0.108), $f(MA) = 0.85$ (0.140) and $f(SF) = 1.10$ (0.114)) are within the range of observed fecundities in the study area (Bregnballe and Gregersen 2003), indicating that the integrated population model is successfully describing the biological processes.

The recruitment probabilities are seen to exhibit a significant downward trend in time (−0.124 (0.020)), implying that cormorants are progressively delaying entering a breeding state. The recruitment rates and breeder survival probabilities are generally lower in the largest of the three colonies, VO. Plots of site- and state-specific survival are shown in Figure 6. Breeder survival is seen to be higher than non-breeder survival at each of the colonies.

Diagnostic goodness-of-fit plots have been examined. The prediction errors resulting from the Kalman filter are tested for normality using QQplots (Figure 7). Plots of log (observed) versus log (expected) for the AS sufficient statistics (McCrea, Morgan, and Bregnballe 2009) are displayed in Figure 8. Neither plot shows evidence of substantial lack of fit.

Table 4 also displays the MLEs from the multivariate normal approximation and diagonal multivariate normal approximation to the mark-recapture likelihood. It is seen for

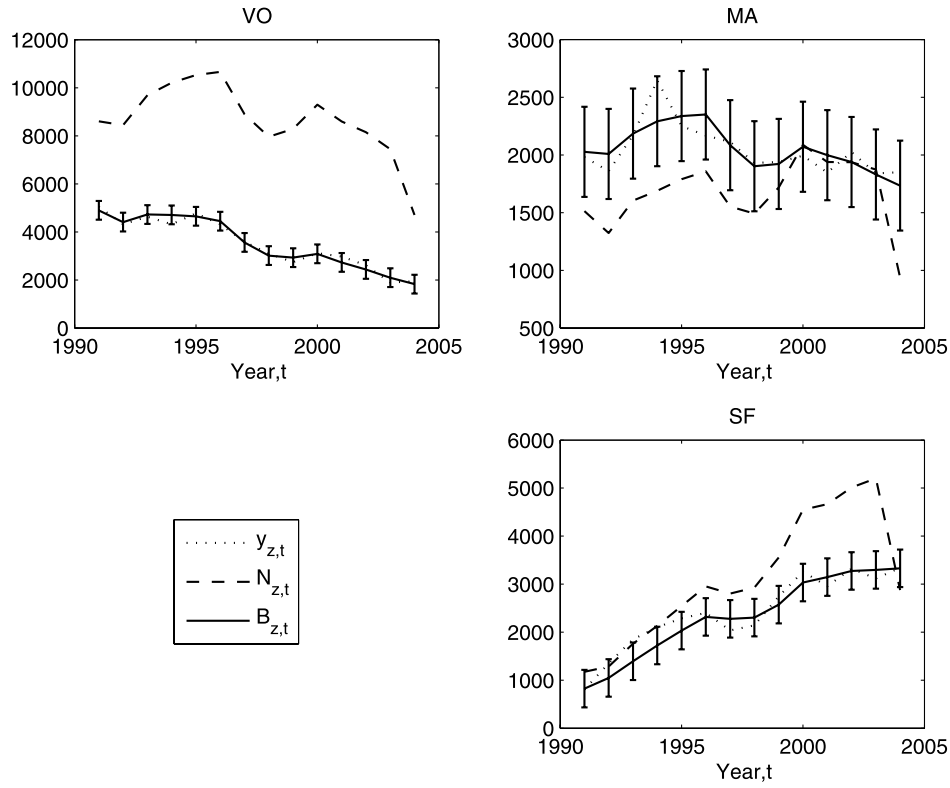

Figure 5. The result of fitting the integrated population model with site- and state- and additive time-dependent survival, departure-site-dependent breeding dispersal, arrival-site-dependent natal dispersal, site and additive time-trend recruitment, site-dependent fecundity and constant observation error. The plots show the observed breeding bird census counts, $y_{z,t}$, (dotted line) and the fitted curve, $\hat{B}_{z,t}$, (solid line) with the estimated observation error, $\hat{\sigma}$, (error bars). The dashed line shows the estimated non-breeding population counts, $\hat{N}_{z,t}$ at site z.

all parameters that the exact and approximate MLEs and SEs are similar, showing in this case that both the multivariate normal approximations are performing well. This was expected from the earlier simulation studies, since the effective sample size of the multi-site mark-recapture cormorant data is large.

5.4. ECOLOGICAL RELEVANCE OF THE RESULTS

Frederiksen and Bregnballe (2001) documented that female cormorants breeding in the VO colony had been observed to delay their first breeding attempt to older ages during the 1990s, which are believed to be the years after the colony size has leveled. These changes occurred during years when the mean breeding success in the colony was declining, and Frederiksen and Bregnballe (2001) suggested that when breeding success starts to decline in a colony because of decreasing food availability it will become less attractive to prospective breeders, which will then join other colonies or delay their first breeding attempt. Similar analyses have not been made for the two other colonies; however, studies indicate that breeding success may also be in decline in these colonies, although starting later than in the VO colony (Bregnballe and Sterup, unpubl.). Figure 5 demonstrates that

Table 4. MLEs on the logistic scale (except for σ on the log scale) from mark-recapture data alone and integrated mark-recapture and census model. Parameter notation follows that in the text; x denotes a non-breeder, whilst X denotes a breeding individual, subscripts denote time dependence ($t - 1990$) and '·' denotes that a parameter is constant over sites. SEs are provided in parentheses.

Parameter	Mark-recapture MLE (SE)	Integrated MLE (SE)	MVN approx and Census MLE (SE)	MVN diagonal approx and Census MLE (SE)
ϕ_1	0.61 (0.31)	0.47 (0.26)	0.45 (0.27)	0.61 (0.31)
ϕ_2	1.20 (0.45)	1.48 (0.24)	1.50 (0.24)	1.55 (0.23)
ϕ_3	0.93 (0.28)	0.60 (0.15)	0.55 (0.15)	0.56 (0.15)
ϕ_4	1.14 (0.27)	1.18 (0.20)	1.20 (0.19)	1.08 (0.18)
ϕ_5	1.22 (0.30)	0.94 (0.16)	0.88 (0.17)	0.92 (0.17)
ϕ_6	0.68 (0.21)	0.91 (0.16)	0.92 (0.14)	0.85 (0.14)
ϕ_7	1.37 (0.36)	0.87 (0.16)	0.80 (0.17)	0.84 (0.17)
ϕ_8	0.30 (0.18)	0.39 (0.12)	0.39 (0.12)	0.36 (0.11)
ϕ_9	0.54 (0.20)	0.58 (0.15)	0.57 (0.15)	0.60 (0.14)
ϕ_{10}	1.11 (0.28)	1.07 (0.21)	1.05 (0.21)	1.09(0.20)
ϕ_{11}	1.39 (0.28)	1.45 (0.23)	1.45 (0.23)	1.49(0.23)
ϕ_{12}	0.80 (0.17)	0.79 (0.14)	0.77 (0.14)	0.80(0.14)
ϕ_{13}	0.82 (0.16)	0.89 (0.14)	0.88 (0.14)	0.85(0.13)
ϕ_{14}	0.97 (0.20)	0.81 (0.15)	0.81 (0.16)	0.77(0.15)
ϕ_{15}	0.64 (0.83)	0.87 (0.19)	0.86 (0.18)	1.07(0.30)
$\phi(MA)$	0.64 (0.18)	0.67 (0.16)	0.66 (0.16)	0.63(0.17)
$\phi(SF)$	0.66 (0.17)	0.67 (0.16)	0.65 (0.16)	0.64(0.16)
$\phi(vo)$	−0.21 (0.10)	−0.12 (0.10)	−0.12 (0.10)	−0.25(0.10)
$\phi(ma)$	−0.38 (0.13)	−0.42 (0.12)	−0.40 (0.12)	−0.39(0.13)
$\phi(sf)$	−0.07 (0.16)	−0.17 (0.15)	−0.15 (0.16)	0.01(0.16)
$\psi(VO, \cdot)$	−4.72 (0.26)	−4.53 (0.23)	−4.53 (0.25)	−4.53 (0.25)
$\psi(MA, \cdot)$	−5.80 (0.66)	−5.65 (0.60)	−5.67 (0.66)	−5.66 (0.66)
$\psi(SF, \cdot)$	−5.92 (0.52)	−5.91 (0.51)	−5.91 (0.52)	−5.93 (0.52)
$\psi(\cdot, ma)$	−4.76 (0.38)	−4.82 (0.39)	−4.79 (0.38)	−4.76 (0.38)
$\psi(\cdot, sf)$	−2.78 (0.16)	−2.67 (0.15)	−2.65 (0.16)	−2.55 (0.16)
$\psi(\cdot, vo)$	−4.74 (0.59)	−4.69 (0.60)	−4.69 (0.59)	−4.74 (0.59)
$\psi(x, X)_{\text{int}}$	−0.67 (0.18)	−0.71 (0.17)	−0.71 (0.17)	−0.76 (0.17)
$\psi(x, X)_{\text{slope}}$	−0.12 (0.02)	−0.12 (0.02)	−0.12 (0.02)	−0.12 (0.02)
$\psi(ma, MA)$	0.88 (0.23)	1.07 (0.22)	1.05 (0.22)	0.87 (0.21)
$\psi(sf, SF)$	0.76 (0.26)	1.01 (0.26)	1.00 (0.25)	1.16 (0.25)
$f(VO)$	–	0.47 (0.07)	0.51 (0.08)	0.70 (0.24)
$f(MA)$	–	−0.16 (0.18)	−0.14 (0.18)	0.02 (0.31)
$f(SF)$	–	0.09 (0.13)	0.11 (0.13)	−0.23 (0.31)
$\sigma(\cdot)$	–	5.28 (0.40)	5.25 (0.40)	5.20 (0.50)

although colony MA may also be in decline, the newest colony, SF, is thriving, exhibiting increasing numbers of breeding and non-breeding individuals. The finding that recruitment rates are declining over time in all three colonies suggests that the conditions for breeding in southwest Kattegat deteriorated during the study period, which is confirmed by data on breeding success as well as total breeding numbers in the region. The poorer conditions might have 'forced' first-time breeders to postpone breeding and/or search for alternative breeding colonies that were located in hitherto less-exploited feeding areas, e.g., because the colonies were younger. Another factor that might have had an influence is that the overall population size of cormorants in Europe increased markedly during the study years

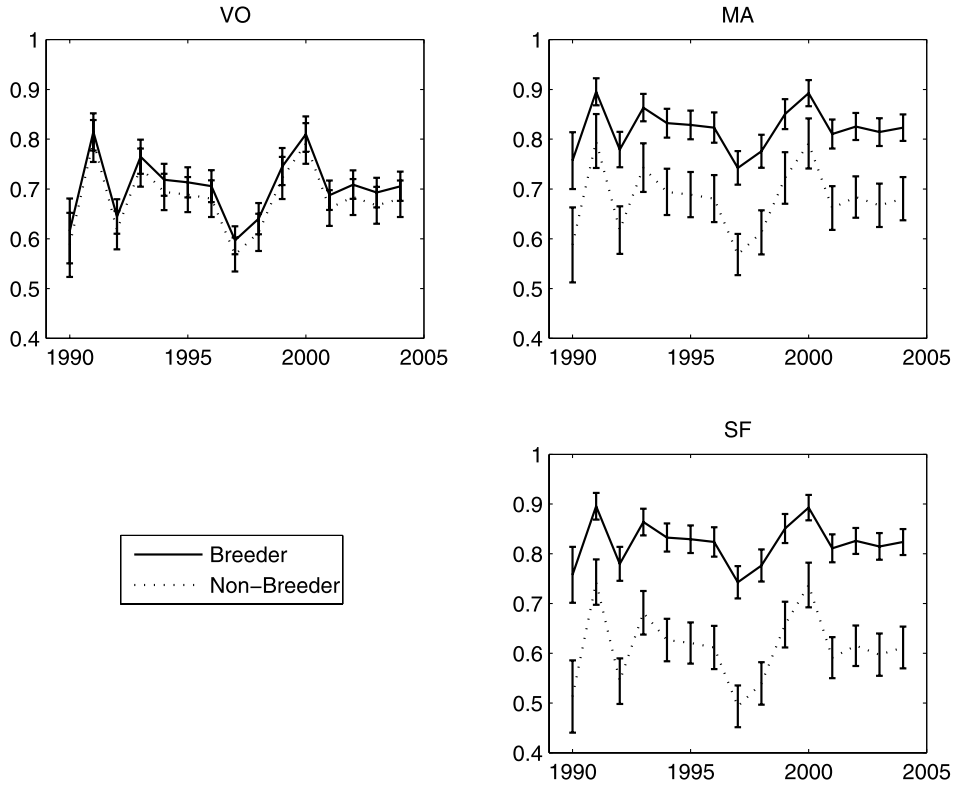

Figure 6. Time-, state- and site-dependent survival estimates from the selected integrated recapture and census model. Approximate 95% confidence intervals are displayed.

and this might have affected competition in wintering and spring staging areas, thereby affecting the body condition attained by 2–4-year-old birds before breeding. We know from plumage observations in the VO colony that the proportion of birds that attained full breeding plumage at age 2–3 years declined during the 1990s (Bregnballe and Gregersen unpubl.), suggesting that the condition of many younger birds was lower than in earlier years.

It was observed that the parameter estimates indicate that breeding survival is higher than non-breeding survival. Bregnballe (2006) found indications for large variation in individual 'quality'; some birds recruited early and reproduced and survived well, whereas others recruited later in life and disappeared sooner from the breeding population. So it is expected that those that attain the age of breeders are on average of better quality than all the individuals that are alive as non-breeders. Studies of distribution of great cormorants in wintering areas (e.g., in Spain and Belgium) show that first-year birds and adults are not distributed evenly within and among feeding areas and roosting sites. This may partly reflect the fact that great cormorants do compete in at least some wintering areas, with the effect that some younger and less experienced birds (probably of lower social status) avoid the feeding and roosting areas dominated by older and more experienced birds. Young and non-breeding birds may utilize feeding areas of lower quality and/or forage at sites where

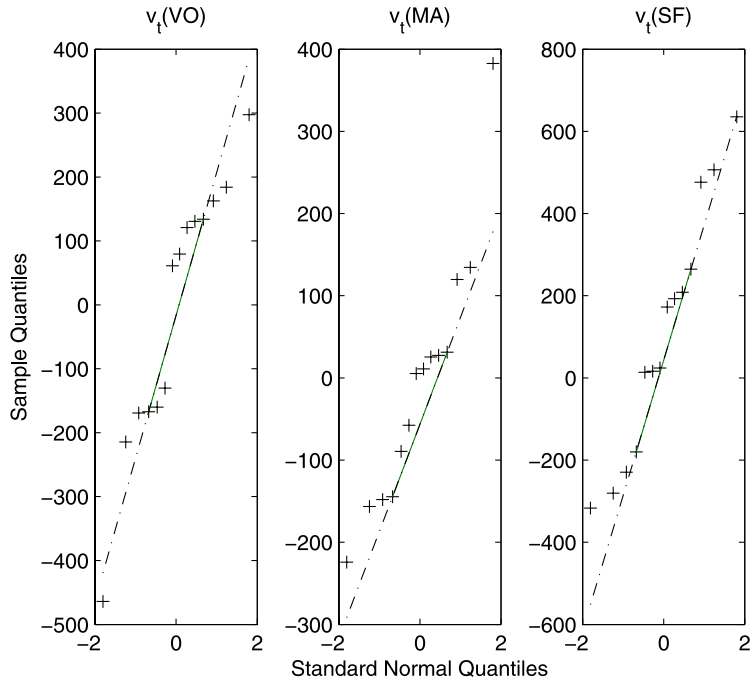

Figure 7. QQplots of the prediction errors v_t obtained from the Kalman filter recursions. Model assumptions expect these errors to be normally distributed.

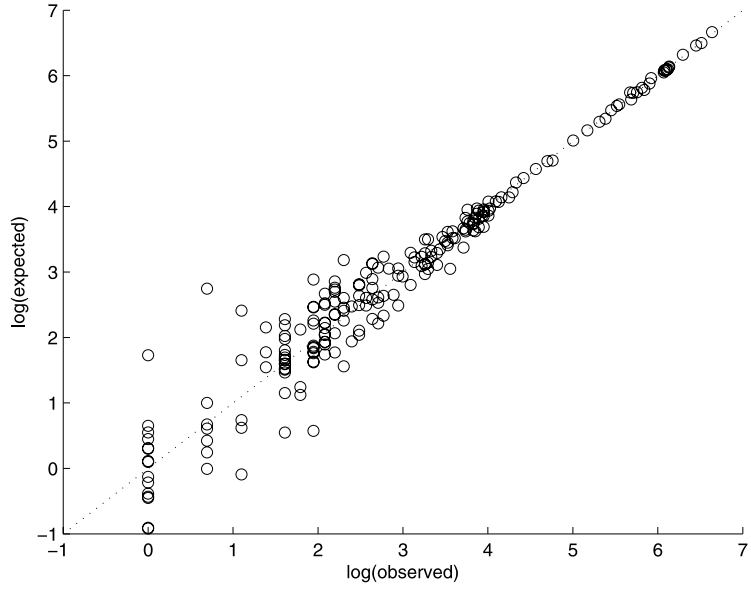

Figure 8. log (observed) versus log (expected) scatter plots for mark-recapture component model.

the risk of mortality is higher (Bregnballe and Frederiksen 2006), for example, because humans shoot great cormorants to reduce conflict with fishery interests.

Natal dispersal was found to be arrival site dependent with a much larger migration towards colony SF than the other two colonies. The SF colony has been more attractive to young birds from VO and MA because of the prospects of breeding with higher success at SF than at VO. Individuals may have emigrated from existing colonies to new colonies because they had obtained knowledge of the spatial variation in environmental quality and had been able to assess that their chances of successful breeding would be higher if they settled outside their natal colony or former breeding colony. Emigration from a larger and older colony may be a response to deteriorating conditions in the colony itself, but may also be a response to the appearance of more prosperous breeding conditions elsewhere. It has been suggested that emigration to a new nearby colony is likely to happen with cormorants if the new colony is located closer to rich and hitherto unexploited or only partly exploited feeding areas (Bregnballe 1995). Thus the distance between a colony and preferred feeding areas can play an important role for the performance of breeding in great cormorants.

The relatively low colonial survival probability of breeding individuals at VO compared to MA and SF may be explained by indications that VO parents were forced to work much harder to find food for the chicks than SF parents. It has been observed that parents at VO fed their chicks less frequently and they also had a higher tendency to abandon their nest in the incubation phase during prolonged periods with hard wind. The difference in survival is not likely to be due to differences between where the birds stay outside the breeding season because the overlap in their distribution outside the breeding season is very high (Bregnballe, Frederiksen, and Gregersen 1997; Bregnballe and Rasmussen 2000).

6. CONCLUSIONS

Integrated population models enable the estimation of coherent demographic and population estimates for compatible data sets. They allow the estimation of important parameters which may have been not estimable, or only estimable to a low degree of precision using the separate data sets. The treatment of the census model in conjunction with the mark-recapture model allows the estimation of population size, as well as the estimation of unobserved classes of the population. Standard population projection matrix models do not achieve this: they treat the population size estimates as deterministic quantities and use the demographic parameters to estimate further parameters such as productivity or fecundity, and do not provide SEs.

When census data are modelled in isolation, parameter estimators will be highly correlated, and this is statistically undesirable. The incorporation of the mark-recapture data reduces these correlations, providing estimators with better properties (Borysiewicz 2008).

In particular, we have seen that by extending integrated population modelling to multistate systems, as well as the above benefits we also witness a distinct improvement in precision for parameters of interest. This improvement is much more appreciable than for previous single-site structures which have been considered.

We have seen through simulation that the multivariate normal approximation to the mark-recapture component likelihood performs well even for relatively small data sets.

Further, we have demonstrated that the diagonal multivariate normal approximation provides an adequate likelihood function which can be optimized in conjunction with further compatible data sets. This will make integrated population modelling even more widely applicable than it is at present, as the diagonal multivariate normal approximation is constructed from only MLEs and their corresponding SEs.

The great cormorant application presented in this paper has demonstrated all of the benefits of multi-site integrated population modelling. As well as improving the precision of site- and state-specific survival probabilities, we have most importantly identified a key trend in the transition probability of recruitment, which has considerable biological interpretation.

SUPPLEMENTAL MATERIALS

A web appendix contains extended simulation results and a note on the computation of standard errors.

ACKNOWLEDGEMENTS

This work was undertaken as part of a NERC-funded Ph.D. studentship and an EPSRC-funded postdoctoral research associate position through the UK-based National Centre for Statistical Ecology. We thank the biologists for their effort in ringing and recording breeding attempts of color-ringed cormorants. We also thank Viviane Hénaux for her comments on an earlier draft of the manuscript, and the associate editor and an anonymous referee for their useful reviews of the paper.

[Accepted March 2010. Published Online June 2010.]

REFERENCES

Arnason, A. N. (1972), "Parameter Estimates from Mark-Recapture-Recovery Experiments on Two Populations Subject to Migration and Death," *Researches on Population Ecology*, 13, 97–113.

Arnason, A. N. (1973), "The Estimation of Population Size, Migration Rates, and Survival in a Stratified Population," *Researches on Population Ecology*, 15, 1–8.

Besbeas, P., and Morgan, B. J. T. (2009), "Integrated Population Model Selection," Technical Report.

Besbeas, P., and Morgan, B. J. T. (2010), "Kalman Filter Initialization for Modelling Population Dynamics," Panagiotis Technical Report UKC/IMS/06/025, SMSAS, University of Kent, UK.

Besbeas, P., Lebreton, J. D., and Morgan, B. J. T. (2003), "The Efficient Integration of Abundance and Demographic Data," *Applied Statistics*, 52, 95–102.

Besbeas, P., Borysiewicz, R. S., and Morgan, B. J. T. (2009), "Completing the Ecological Jigsaw," *Environmental and Ecological Statistics*, 3, 513–540. Edited by Thomson, D. L., Cooch, E. G., and Conroy, M. J.

Besbeas, P., Freeman, S. N., Morgan, B. J. T., and Catchpole, E. A. (2002), "Integrating Mark-Recapture-Recovery and Census Data to Estimate Animal Abundance and Demographic Parameters," *Biometrics*, 58, 540–547.

Borysiewicz, R. S. (2008), "The Combined Analysis of Multi-Site Mark-Recapture-Recovery Data and Multi-Site Census Data," Ph.D. thesis, University of Kent.

Borysiewicz, R. S., Morgan, B. J. T., Hénaux, V., Bregnballe, T., Lebreton, J. D., and Gimenez, O. (2009), "An Integrated Analysis of Multi-Site Recruitment, Mark-Recapture-Recovery and Multi-Site Census Data," *Environmental and Ecological Statistics*, 3, 579–591. Edited by Thomson, D. L., Cooch, E. G., and Conroy, M. J.

Bregnballe, T. (1995), "Cormorant Research in Denmark," *Cormorant Research Group Bulletin*, 1, 4–7.

Bregnballe, T. (2006), "Age-Related Fledgling Production in Great Cormorants Phalacrocorax Carbo: Influence of Individual Competence and Disappearance of Phenotypes," *Journal of Avian Biology*, 37, 149–157.

Bregnballe, T., and Frederiksen, M. (2006), "Net-Entrapment of Great Cormorants Phalacrocorax Carbo Sinensis in Relation to Age and Population Size," *Wildlife Biology*, 12, 143–150.

Bregnballe, T., and Gregersen, J. (2003), "Within-Colony Variation in Breeding Success in a Great Cormorant Colony in Denmark," *Die Vogelwelt*, 124, 115–122.

Bregnballe, T., and Rasmussen, T. (2000), "Post-Breeding Dispersal of Great Cormorants Phalacrocorax Carbo Sinensis from Danish Breeding Colonies," *Dansk Ornitologisk Forenings Tidsskrift*, 94, 175–187.

Bregnballe, T., Frederiksen, M., and Gregersen, J. (1997), "Seasonal Distribution and Timing of Migration of Cormorants Phalacrocorax Carbo Sinensis Breeding in Denmark," *Bird Study*, 44, 257–276.

Brownie, C., Hines, J. E., Nichols, J. D., Pollock, K. H., and Hestbeck, J. B. (1993), "Capture-Recapture Studies for Multiple Strata Including Non-Markovian Transitions," *Biometrics*, 49, 1173–1187.

Buckland, S. T., Newman, K. B., Thomas, L., and Koesters, N. B. (2004), "State Space Models for the Dynamics of Wild Animal Populations," *Ecological Modelling*, 171, 157–175.

Burnham, K. P., and Anderson, D. R. (2002), *Model Selection and Multimodel Inference: A Practical Information Theoretic Approach* (2nd ed.), New York: Springer.

Caswell, H. (2000) *Matrix Population Models: Construction, Analysis and Interpretation* (2nd ed.), Sunderland: Sinauer.

Choquet, R., Reboulet, A. M., Pradel, R., Gimenez, O., and Lebreton, J. D. (2003), User's Manual for U-Care, Mimeographed document, CEFE/CNRS, Montpellier, France.

Choquet, R., Reboulet, A. M., Pradel, R., Gimenez, O., and Lebreton, J. D. (2004), "M-Surge: New Software Specifically Designed for Multistate Capture-Recapture Models," *Animal Biodiversity and Conservation*, 27, 207–215.

Cormack, R. M. (1964), "Estimates of Survival from Sightings of Marked Animals," *Biometrika*, 51, 429–438.

Durbin, J., and Koopman, S. J. (2001), *Time Series Analysis by State Space Methods*, Oxford: Oxford University Press.

Frederiksen, M., and Bregnballe, T. (2001), "Conspecific Reproductive Success Affects Age of Recruitment in a Great Cormorant, Phalacrocorax Carbo Sinensis, Colony," *Proceedings of the Royal Society of London: Biological Sciences*, 268, 1519–1526.

Frederiksen, M., Lebreton, J. D., and Bregnballe, T. (2001), "The Interplay Between Culling and Density-Dependence in the Great Cormorant: A Modelling Approach," *Journal of Applied Ecology*, 38, 617–627.

Gauthier, G., Besbeas, P., Lebreton, J. D., and Morgan, B. J. T. (2007), "Population Growth in Greater Snow Geese: A Modeling Approach to Integrating Demographic and Population Survey Information," *Ecology*, 88, 1420–1429.

Harvey, A. C. (1989), *Forecasting, Structural Time Series Models and the Kalman Filter*, Cambridge: Cambridge University Press.

Hénaux, V., Bregnballe, T., and Lebreton, J. D. (2007), "Dispersal and Recruitment During Population Growth in a Colonial Bird, the Great Cormorant," *Journal of Avian Biology*, 38, 44–57.

Jolly, G. M. (1965), "Explicit Estimates from Capture-Recapture Data with Both Death and Imigration-Stochastic Models," *Biometrika*, 52, 225–247.

Lebreton, J.-D., Almeras, T., and Pradel, R. (1999), "Competing Events, Mixtures of Information and Multistratum Recapture Models," *Bird Study*, 46, S39–S46.

McCrea, R. S., Morgan, B. J. T. and Bregnballe, T. (2009), "One Size Fits All?," Technical Report UKC/IMS/09/032, IMSAS, University of Kent, UK.

McCrea, R. S., and Morgan, B. J. T. (2010), "Multi-Site Mark-Recapture Model Selection Using Score Tests," Biometrics. doi:*10.1111/j.1541-0420.2010.01421.x*.

Newman, K. B., Buckland, S. T., Lindley, S. T., Thomas, L., and Fernandez, C. (2006), "Hidden Process Models for Animal Population Dynamics," *Ecological Applications*, 16, 74–86.

Reynolds, T. J., King, R., Harwood, J., Frederiksen, M., Harris, M. P., and Wanless, S. (2009), "Integrated Data Analysis in the Presence of Emigration and Tag Loss," *Journal of Agricultural, Biological and Environmental Statistics*, 14, 411–431.

Schaub, M., Gimenez, O., Sierro, S., and Arlettaz (2007), "Assessing Population Dynamics from Limited Data with Integrated Modeling: Life History of the Endangered Greater Horseshoe Bat," *Conservation Biology*, 21, 945–955.

Schwarz, C. G., Schweigert, J. F., and Arnason, A. N. (1993), "Estimating Migration Rates Using Tag-Recovery Data," *Biometrics*, 59, 291–318.

Seber, G. A. F. (1965), "A Note on the Multiple-Recapture Census," *Biometrika*, 52, 249–259.

Tavecchia, G., Besbeas, P., Morgan, B. J. T., and Coulson, T. (2009), "Hidden Demographic Processes and Population Estimates Through State-Space Modelling," *American Naturalist*, 173, 722–733.

White, G. C., and Burnham, K. P. (1999), "Program MARK: Survival Estimation from Populations of Marked Animals," *Bird Study*, 46, S120–S138.

Williams, B. K., Nichols, J. D., and Conroy, M. J. (2001) *Analysis and Management of Animal Populations*, San Diego: Academic Press.